(Received 8 January 2026, Accepted 16 March 2026, Scheduled 1 April 2026)

Fabry-Perot Resonator Antenna Design Based on Phased Array Feed

Zechen Li[1,*], Zibin Weng[1,2], Yahong Li[1], Youqian Su[1], and Jingnan Guo[1]

[1] *Hangzhou Institute of Technology, Xidian University, Hangzhou 311231, Zhejiang, China*
[2] *National Key Laboratory of Radar Detection and Sensing, Xidian University, Xi'an 710071, Shaanxi, China*

ABSTRACT: To address the issues of narrow gain bandwidth and severe element coupling faced by traditional Fabry-Perot resonant antennas in phased-array feed systems, this paper proposes a decoupling design method based on a highly optimized resonant mode height. By analyzing the electric field distributions and coupling mechanisms under multi-feed conditions, an improved resonator height calculation formula suitable for phased-array feeds was derived, achieving mutual suppression of energy between reflected wave coupling and inter-element coupling. A 2×2 microstrip antenna array is used as the feed source. Combined with a multilayer positive phase gradient partially reflective surface, a Fabry-Perot antenna prototype operating at 28 GHz was designed and fabricated. Simulated and experimental results demonstrate that compared to conventional designs, this antenna achieves a maximum gain at 28 GHz, increased from 21.80 dBi to 23.15 dBi, with the 3-dB gain bandwidth expanded from 1350 MHz to 1730 MHz. This study provides an effective approach for achieving a broadband high-gain design in phased-array fed Fabry-Perot resonant antennas.

1. INTRODUCTION

Driven by the new generation information technology revolution [1, 2], communication systems are making leaps toward high-speed, long-distance, and wide-coverage capabilities [3], whether it is a high-reliability real-time interconnection of 5G/6G IoT devices [4] or high-capacity, precise coverage transmission in the millimeter-wave band [5, 6]. Both impose stringent requirements on the antenna performance, including high gain, wide bandwidth, and strong directionality [7]. Owing to their limited gain, traditional microstrip antennas are no longer sufficient to meet the demands of the aforementioned application scenarios [8, 9]. Fabry-Perot resonator antennas, which utilize a resonant structure formed by a partially reflective surface and ground plane, can significantly enhance the directional gain of the antenna. Consequently, they represent an effective technical approach for realizing high-performance millimeter-wave communication antennas [10, 11].

In 1956, Trentini first proposed a Fabry-Perot resonator antenna design [12]. This antenna employs a resonant cavity structure formed by placing a portion of the reflector parallel to the metal ground plane. Utilizing multiple reflections of electromagnetic waves between the two surfaces significantly enhances the directional gain of the antenna, with experimentally measured gains reaching approximately 14 dBi. This pioneering study laid an important foundation for the development of high-gain antennas. In 2014, Konstantinidis et al. proposed a broadband Fabry-Perot resonator antenna based on a three-layer partially reflective surface [13]. This antenna employed a waveguide-fed slot as the feed source. The design integrates theoretical approaches from equivalent circuit modeling and full-wave analysis of periodic structures. By constructing a reflection characteristic with a positive phase gradient, it achieves broadband linear variation of the reflection phase with frequency, thereby effectively expanding the bandwidth of the antenna. The simulated and experimental results indicate that this antenna achieves a maximum gain exceeding 20 dBi, with a 3-dB gain bandwidth of approximately 14.5%. It significantly enhances the overall performance of traditional Fabry-Perot antennas in terms of bandwidth and gain. However, this design methodology is not applicable to array feed structures. For array feed design, in 2016, Qin et al. proposed a co-calibrated dual-frequency, dual-polarization, high-gain F-P resonator antenna for synthetic aperture radar [14], wherein the feed section consisted of a central C-band patch and a peripheral 2×2 X-band patch array. Furthermore, by increasing the X-band unit spacing to 40 mm, the mutual coupling between units was effectively suppressed. The test results indicate that the antenna achieves a gain of approximately 16.2 dBi in the C-band and approximately 20.8 dBi in the X-band. The aforementioned research has propelled the advancement of Fabry-Perot resonator antennas, not only extending traditional waveguide feeders into array feeders but also proposing effective methods to suppress the coupling between feeders. Building on this work, we introduce a novel array feeder decoupling technique.

This study designed a high-gain Fabry-Perot resonator antenna based on a 2×2 phased-array feed. To address the coupling issues among multiple array elements, we optimized the height relationship between the feed and array planes. By adjusting the spacing between certain reflectors and the phased-array feed, the height was increased from $h_1 = 4.5$ mm to $h_2 = 10.1$ mm. Modifying the propagation path loss causes the coupling between array elements to cancel out the energy coupled by the reflected waves, thereby achieving gain enhancement. At the 28 GHz frequency point, the antenna's maximum gain increased from 21.80 dBi to 23.15 dBi, representing a 1.35 dB gain improvement. The 3-dB bandwidth expanded

* Corresponding author: Zechen Li (13105345464@163.com).

from 1350 MHz to 1730 MHz. The simulation results were aligned with those of physical testing, validating the reliability of this design.

2. ANTENNA GEOMETRY AND ANALYSIS

Figure 1 shows a schematic of the Fabry-Perot resonator antenna structure. A partially reflective surface (PRS) was positioned above the 2×2 phased-array feed antenna. This surface, together with the floor of the phased-array feed, forms a resonator cavity. The electromagnetic waves radiated by the microstrip feed antenna underwent multiple reflections and transmissions within the cavity. When the cavity satisfies specific resonance conditions, the electromagnetic waves passing through the PRS achieve in-phase superposition, thereby enhancing the antenna gain and narrowing the beamwidth. The distance between the microstrip phased-array antenna and PRS is h. The feed section employed a 2×2 microstrip antenna array. Figure 2 shows the cross-sectional structure of each layer of the Fabry-Perot resonator antenna, with an element spacing of $L_t = W_t = 4.2$ mm. Each microstrip antenna had dimensions of $b_1 = c_1 = 1.73$ mm. The PRS consists of a 7×7 array of positive-phase gradient elements, with peripheral areas reserved for mechanical connection structures. The overall dimensions of the PRS are $L = W = 60$ mm.

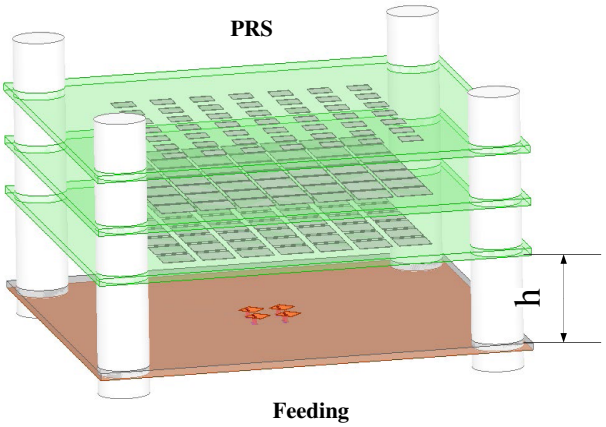

FIGURE 1. Schematic diagram of Fabry-Perot resonator antenna structure.

Figure 3 shows the unit structure and simulation results for a partially reflective surface. This unit employs a classic positive phase gradient design, in which the phase increases with frequency while maintaining a stable amplitude within the phase variation range. As illustrated, the unit employs a TLX-8 dielectric substrate ($\varepsilon_r = 2.55$, thickness $L_3 = 0.787$ mm) with a square pattern featuring the following dimensions: $L_1 = 4.67$ mm, $L_2 = 4.9$ mm, period $P = 5.4$ mm, and $a_1 = 4.49$ mm, $a_2 = 4.90$ mm, and $a_3 = 2.75$ mm. Within the 28.5 GHz to 30.4 GHz frequency band, the unit's phase increases monotonically from $-18°$ to $23°$, while the amplitude remains essentially stable at approximately -5 dB.

3. ANTENNA THEORY ANALYSIS

Figure 4 illustrates a schematic diagram of the Fabry-Perot theoretical analysis structure. Assuming the reflection coefficient $\rho e^{j\varphi}$ of a portion of the emitting surface, where ρ represents the reflection amplitude, and φ denotes the reflection phase. The amplitude of ray n (where n is a positive integer) is proportional to $\rho^n\sqrt{1-\rho^2}$, and the phase difference between rays n and 0 can be obtained as

$$\Delta_n = n\phi = n\left[\varphi - \pi - \frac{4\pi}{\lambda}h\cos\theta\right] \tag{1}$$

The far-field electric field can be obtained as

$$\vec{E} = \sum_{n=0}^{\infty} F(\theta)E_0\rho^n\sqrt{1-\rho^2}e^{j\Delta_n} \tag{2}$$

The far-field energy pattern of the antenna is

$$S(\theta,\phi) = \frac{1-\rho^2}{1+\rho^2-2\rho\cos\left(\varphi-\pi-\frac{4\pi}{\lambda}h\cos\theta\right)}F^2(\theta,\phi) \tag{3}$$

Under normal circumstances, the maximum radiation direction of a Fabry-Perot resonator antenna is along the measurement direction, at $\theta = 0$. At this point, if the resonator cavity height h satisfies the condition shown in Equation (5), the amplitude of the far-field energy pattern exhibits its maximum value. Thus, the cavity height h represents the resonance condition of the antenna.

$$\varphi - \pi - \frac{4\pi}{\lambda}h = -2N\pi \tag{4}$$

$$h = \left(\frac{\varphi}{2\pi} - \frac{1}{2}\right)\frac{\lambda}{2} + N\frac{\lambda}{2}, \quad N = 0, 1, 2, \ldots \tag{5}$$

φ is the reflection phase of the PRS unit, and λ is the wavelength at the corresponding frequency. Fabry-Perot resonator antennas typically have a fixed structure (i.e., h remains constant). As f increases, the reflection phase φ must correspondingly increase to satisfy the resonance conditions and achieve broadband operation. Based on the height formula characteristics of the Fabry-Perot resonator, this antenna generally operates at different resonance orders. The operational bandwidth was broadened by adjusting the phase to match the frequency variations.

Figure 5 shows the structural diagram of the Fabry-Perot phased-array feed and its corresponding electric field distribution. Analysis of the electric field distribution for different numbers of feeds revealed that the electric field strength gradually decreased with increasing distance from the antenna. Notably, the electric field attenuation rate for the 2×2 phased-array feed was significantly slower than that of a conventional microstrip antenna, and the electric field distribution remained relatively stable within a half-wavelength height range.

In conventional single-feed Fabry-Perot resonant cavity antennas, the cavity height is typically limited to $h \leq \lambda/2$ to maintain satisfactory gain, as the electric field coupled into

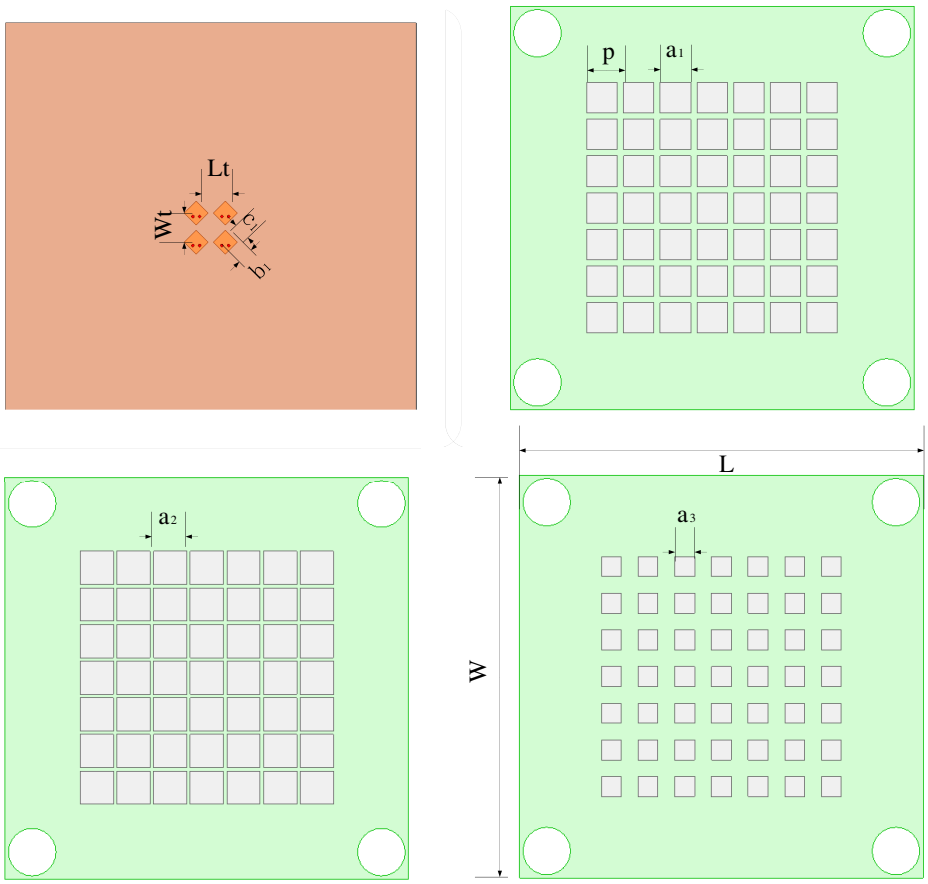

FIGURE 2. Cross-sectional diagram of each layer in the Fabry-Perot resonator antenna.

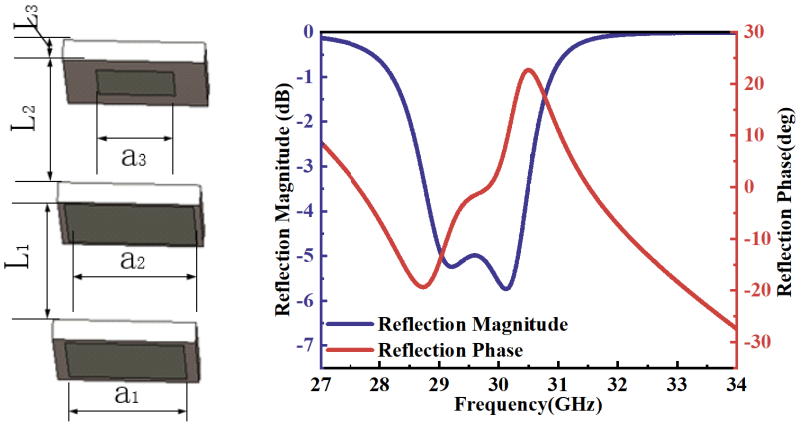

FIGURE 3. Schematic diagram of partial reflective surface unit and simulation results.

the cavity attenuates rapidly with increasing height for a single feed source. However, when a phased array is employed as the feed, the mutual coupling between array elements and the coupling between reflected waves and the feed introduce additional phase variations and energy losses, significantly affecting the in-phase superposition condition within the cavity. A review of the literature reveals that few studies have proposed modified analytical formulas accounting for such complex coupling scenarios in array-fed configurations.

To address this gap, we conducted extensive full-wave simulations using High Frequency Structure Simulator (HFSS) to investigate the optimal cavity height for various array configurations. The results indicate that as the number of feed elements increases, the electric field intensity decays more slowly with height. Based on these observations and physical reasoning, we proposed the modified resonance condition given in Equation (6). The additional term $\lambda/2\lfloor M-1\rfloor$ is introduced to empirically account for the equivalent path length increase caused by the combined effects of inter-element coupling and reflected-wave coupling.

Figure 6 presents a theoretical analysis of Fabry-Perot resonator antenna coupling. In Fabry-Perot resonators employ-

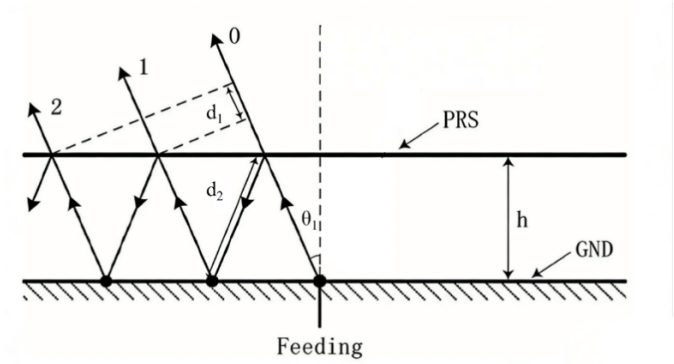

FIGURE 4. Schematic diagram of the Fabry-Perot theoretical analysis structure.

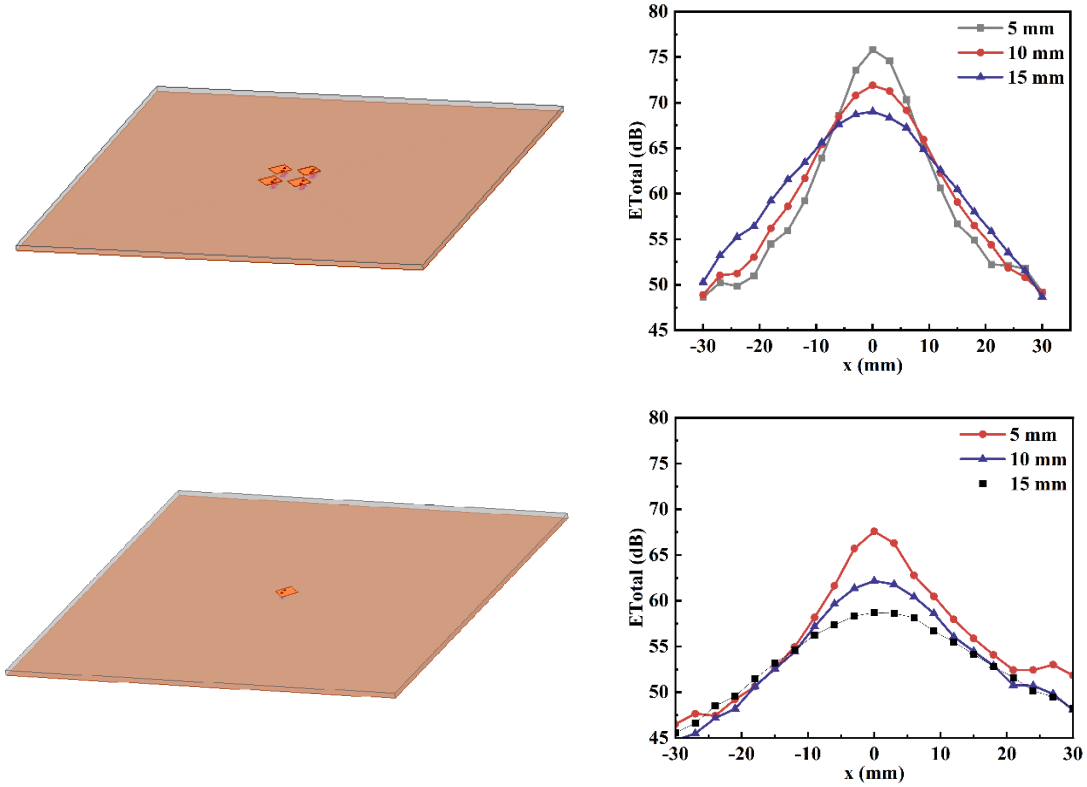

FIGURE 5. Schematic of phased-array feed structure and corresponding electric field distribution.

ing phased array antennas as feed sources, the gain enhancement effect is typically inferior to that achieved with single microstrip Fabry-Perot resonator antennas because of the mutual coupling between array elements and the coupling between reflected waves and the feed source. To address this, this study proposes a coupling adjustment method: by altering the height of the partial reflector surface relative to the phased-array feed (from h_1 to h_2), the electromagnetic wave propagation path and path loss can be adjusted. This causes the energy from the element-to-element coupling and reflected wave coupling to cancel each other out, thereby improving the gain. Correspondingly, for an $M \times M$ array feed, the modified resonance condition formula is as follows:

$$h = \left(\frac{\varphi}{2\pi} - \frac{1}{2} + N\right)\frac{\lambda}{2} + \frac{\lambda}{2}\lfloor M-1 \rfloor \tag{6}$$

Here, $\lfloor\ \rfloor$ denotes the floor function operator; M represents the number of rows (or columns) in the phased-array feed; and N is the adjustment coefficient. Condition $\varphi/(2\pi) - 1/2 + N$ must yield a value greater than zero, with N being the smallest positive integer satisfying this requirement.

4. FABRY-PEROT RESONATOR ANTENNA DESIGN, FABRICATION AND MEASUREMENTS

To validate the performance of the array antenna as a feed source, this study employed HFSS software for modeling and simulation, followed by the testing and analysis of its radiation characteristics. Using conventional design methods, the calculation yields $h_1 = 4.82$ mm according to Equation (5). After comprehensively evaluating metrics such as 3 dB bandwidth and maximum gain, the optimal antenna performance

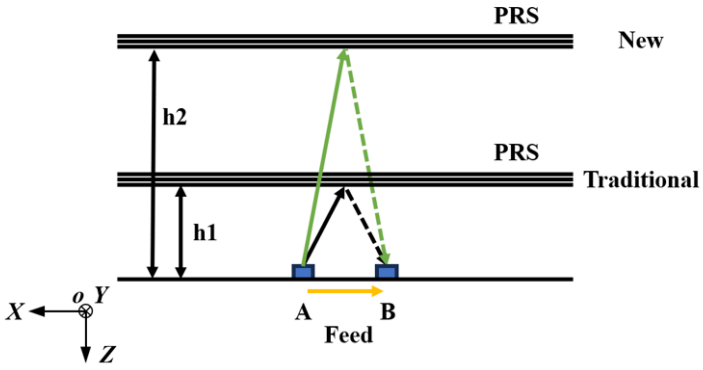

FIGURE 6. Theoretical analysis of Fabry-Perot resonator antenna coupling.

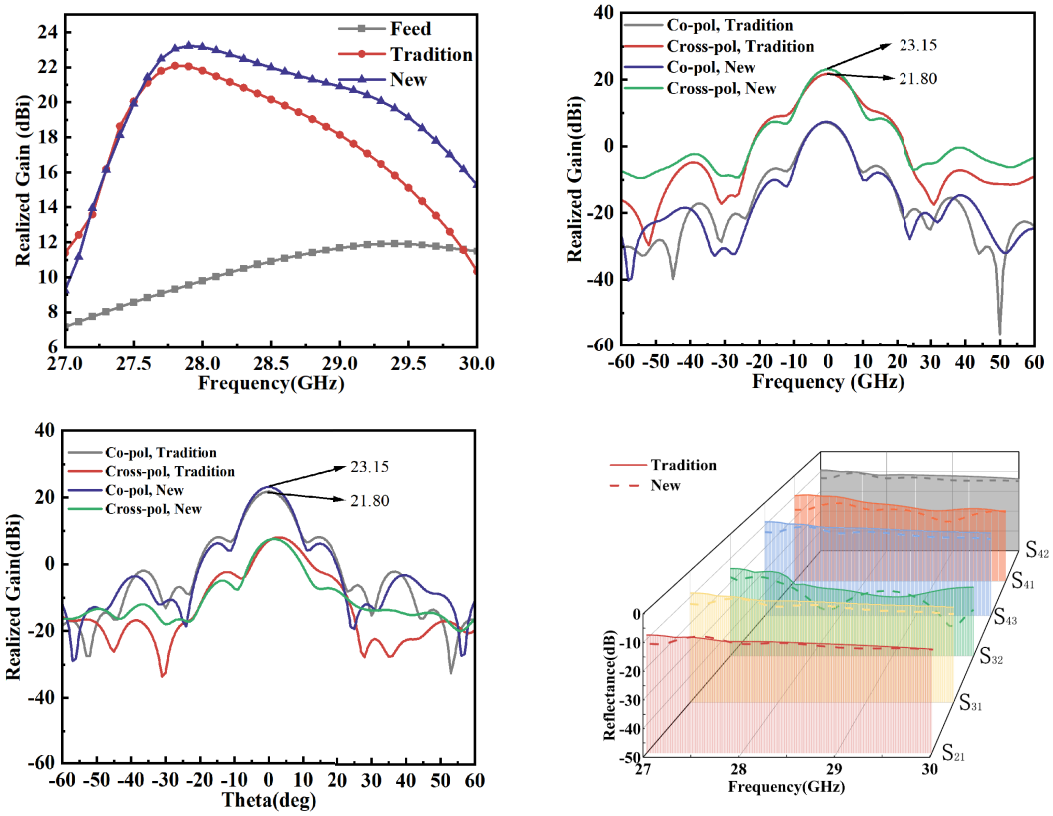

FIGURE 7. Simulation results of Fabry-Perot resonator antenna.

at 28 GHz was determined to occur at $h_1 = 4.5$ mm. Subsequently, the design was performed using the improved formula (6), yielding a reflection phase $\varphi = -18°$ $(-\pi/10)$. Given an operating wavelength $\lambda = 10.714$ mm, where $\varphi/(2\pi) - 1/2 + M$ is positive and $\varphi/(2\pi) - 1/2 < 0$, h_2 was calculated as 10.1 mm, resulting in a total antenna height of 23 mm.

Figure 7 illustrates a gain comparison between the two designs. Simulation results show that the gain at 28 GHz increases from 21.80 dBi to 23.16 dBi, representing a 1.35 dB improvement. The 3-dB bandwidth expands from 1350 MHz to 1730 MHz. Comparing the S-parameters of both designs reveals that within the 27.5 GHz–30 GHz band, the improved solution exhibits lower S-parameters than the traditional design, demonstrating superior matching characteristics.

Figure 8 shows the electric field distribution of the Fabry-Perot resonator antenna. For the proposed design, (a) and (b) depict the electric field distributions on the aperture and at the feed plane, respectively; (c) and (d) show the corresponding distributions for the conventional design.

A comparison of Figs. 8(a) and (c) reveals that the proposed design achieves a more uniform and stronger electric field distribution across the aperture. Furthermore, by comparing (b) and (d), it can be observed that in the proposed design, the cancellation between reflected-wave coupling and inter-element coupling leads to a higher field intensity at the feed plane,

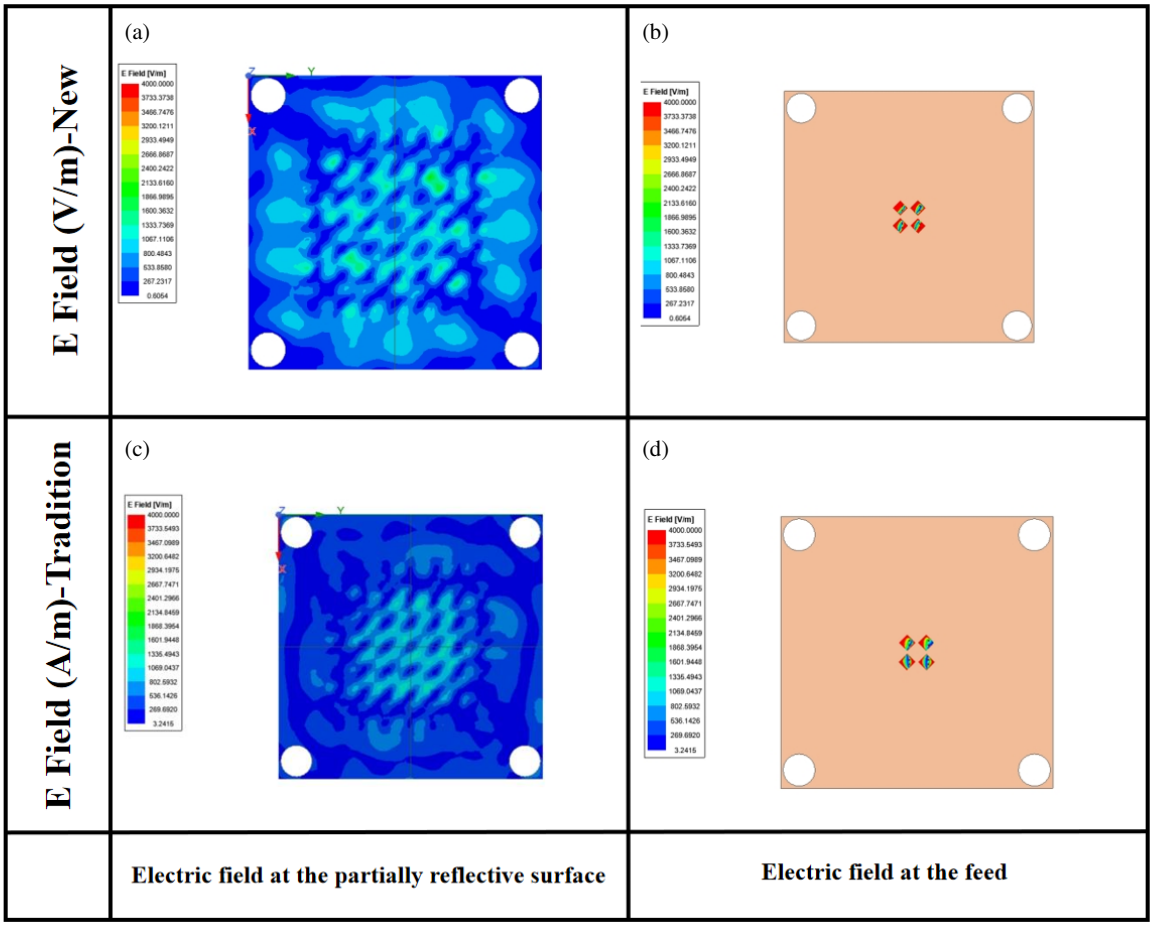

FIGURE 8. Electric field distribution of the Fabry-Perot resonator antenna.

TABLE 1. Comparison of simulated and measured results.

Parameter	Simulated	Measured
Gain/dBi	23.15	22.60
3-dB Bandwidth/MHz	1730 MHz	1690 MHz
10-dB beamwidth/°	9.7°	10.1°
Radiation Efficiency	52.4%	46.8%
Sidelobe Level/dB	−14.8	−16.2

as well as a more uniform distribution among the individual feed elements. This validates that the proposed scheme enables the desired coupling cancellation, thereby achieving significant gain enhancement.

Figure 9 shows the fabrication and measurements of the Fabry-Perot resonator antenna. The fabricated antenna was tested in a far-field microwave anechoic chamber, and the gain test results are shown in Figure 10. The actual test data indicate that at the 28 GHz frequency point, the feed antenna gain was 9.6 dBi. After loading with the Fabry-Perot resonator cavity, the gain increases to 22.6 dBi, representing a relative improvement of approximately 13 dB. The 3 dB bandwidth was 1.79 GHz (27.57 GHz to 29.26 GHz). Comparing the measured and simulated results, the measured pattern exhibited deviations from the simulation, primarily attributed to height irregularities caused by the screw-nut assembly and manufacturing tolerances. These factors contributed to measurement errors in both the gain and pattern. As detailed in Table 1, Figure 10 shows the comparison between the measured normalized radiation pattern and HFSS simulated radiation pattern. Overall, the two align well, validating the reliability of the simulation model.

To evaluate the performance of the proposed design further, several Fabry-Perot resonator antenna designs with array feed sources are summarized in Table 2. It can be seen that the proposed design method achieves a realized gain of 22.6 dBi and

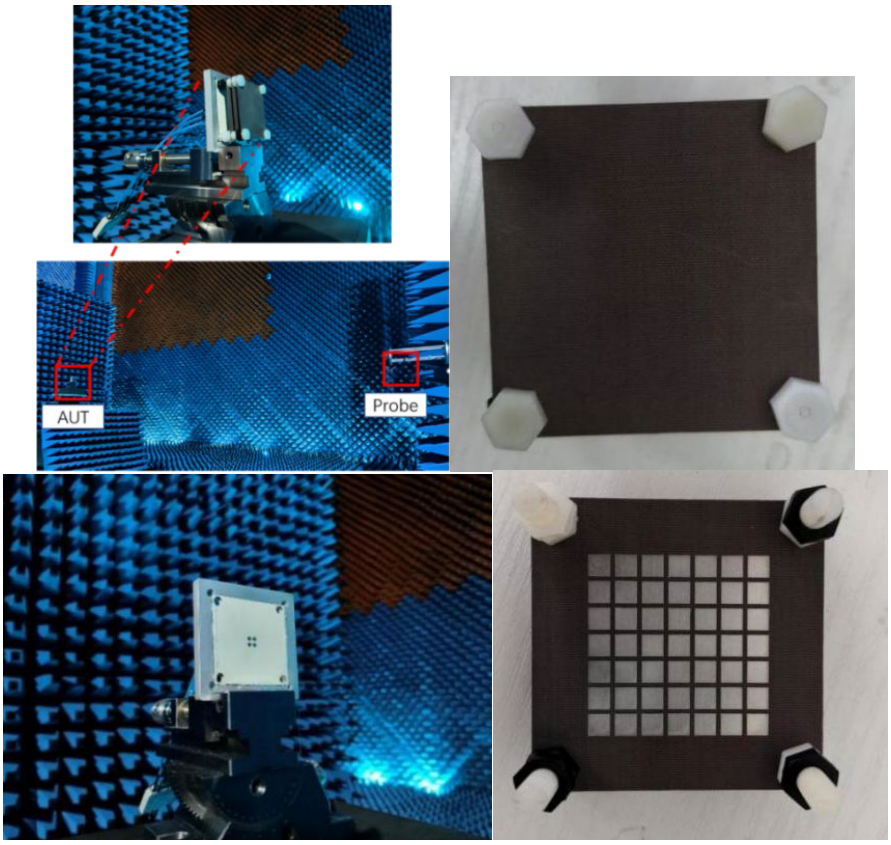

FIGURE 9. Physical Fabry-Perot resonator antenna and anechoic chamber measurement diagram.

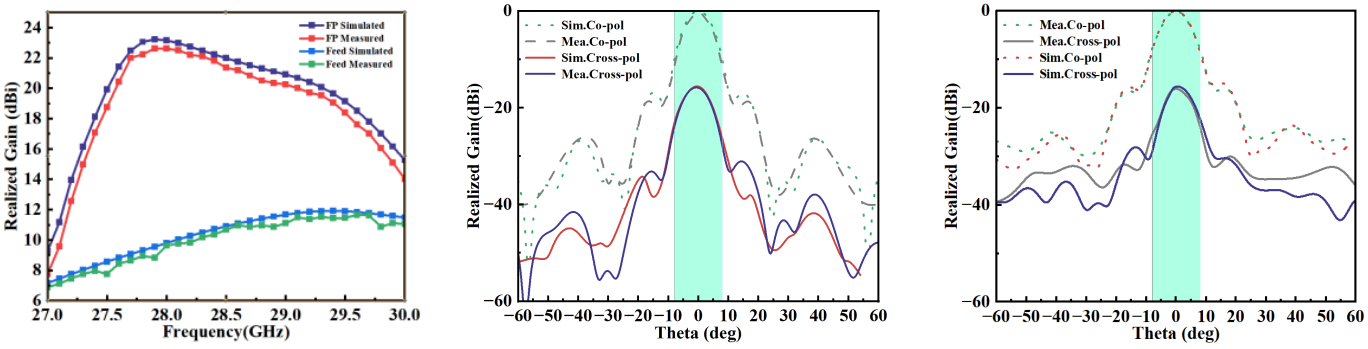

FIGURE 10. Comparison of simulated and actual fabricated antennas for this design diagram.

TABLE 2. A comparison of the proposed antenna and reported designs.

Reference	Frequency (GHz)	Realized Gain (dBi)	3-dB bandwidth (dB)	Gain Enhancement (dB)	Feeding
[13]	14	20.8	15%	/	Waveguide
[18]	27.7	24	9.6	10.1	waveguide (SIW)
[19]	10.25	12	/	8.9	1 × 1 patch antenna
[16]	10	18.1	/	3.0	1 × 8 array antenna
[17]	11	14.33	5.36	/	1 × 2 array antenna
[14]	9.6	20	6.3	7.9	2 × 2 array antenna
[15]	14	19	5.7%	7.1	2 × 2 array antenna
This Work	28	22.6	6.4%	13.0	2 × 2 array antenna

a gain enhancement of 13 dBi, demonstrating a superior gain enhancement capability compared to the feed source.

5. CONCLUSION

This study designs a high-gain Fabry-Perot resonator antenna based on a 2×2 phased-array feed. Based on an improved resonance condition formula, this paper proposes a method to suppress coupling by optimizing the spacing between the partial reflector and feed. The propagation path loss was effectively altered by optimizing the height from $h_1 = 4.5$ mm to $h_2 = 10.1$ mm, and the propagation path loss was effectively altered. This caused the coupling between the array elements and the coupling energy of the reflected waves to cancel each other out, significantly enhancing the antenna performance.

The experimental results demonstrate that at 28 GHz, the antenna's maximum gain increases from 21.80 dBi to 23.15 dBi — a 1.35 dB improvement — while the 3-dB bandwidth expands from 1350 MHz to 1730 MHz. The simulation results agree well with the experimental measurements, validating the effectiveness and design reliability of the proposed method. This work provides a feasible optimization approach for enhancing the gain and bandwidth of phased-array fed Fabry-Perot antennas, offering promising applications in millimeter-wave communication and radar systems.

REFERENCES

[1] Pichot, C., G. H. Huff, Y. Yang, Z. H. Jiang, X. Tong, T. H. Loh, A. Alemaryeen, M. Wagih, S. Noghanian, R. C. Paryani, Y. Huang, K. Sakakibara, F. Vipiana, E. Fear, S. C. Bakshi, R. Waterhouse, J. Urbina, S. D. Meinrath, B. P.-J. Shih, R. Sharma, V. Manohar, F. T. Dagefu, and K. Ito, "New and emerging directions in the fields of antennas and propagation," *IEEE Transactions on Antennas and Propagation*, Vol. 73, No. 1, 566–581, Jan. 2025.

[2] Jabbar, A., Q. H. Abbasi, N. Anjum, T. Kalsoom, N. Ramzan, S. Ahmed, P. M. Rafi-Ul-Shan, O. P. Falade, M. A. Imran, and M. U. Rehman, "Millimeter-wave smart antenna solutions for URLLC in industry 4.0 and beyond," *Sensors*, Vol. 22, No. 7, 2688, 2022.

[3] Yu, X., J. Zhang, M. Haenggi, and K. B. Letaief, "Coverage analysis for millimeter wave networks: The impact of directional antenna arrays," *IEEE Journal on Selected Areas in Communications*, Vol. 35, No. 7, 1498–1512, Jul. 2017.

[4] Wang, X., L. Kong, F. Kong, F. Qiu, M. Xia, S. Arnon, and G. Chen, "Millimeter wave communication: A comprehensive survey," *IEEE Communications Surveys & Tutorials*, Vol. 20, No. 3, 1616–1653, 2018.

[5] Kumar, S., A. S. Dixit, R. R. Malekar, H. D. Raut, and L. K. Shevada, "Fifth generation antennas: A comprehensive review of design and performance enhancement techniques," *IEEE Access*, Vol. 8, 163 568–163 593, 2020.

[6] Jahanbakhsh Basherlou, H., N. O. Parchin, and C. H. See, "Antenna design and optimization for 5G, 6G, and IoT," *Sensors*, Vol. 25, No. 5, 1494, 2025.

[7] Peter, I. and S. S. Singhwal, *5G Antenna Materials and Ensuing Challenges*, L. Matekovits, B. K. Kanaujia, J. Kishor, S. K. Gupta (eds.), Printed Antennas for 5G Networks, PoliTO Springer Series, Springer, Cham, 2022.

[8] Ullah, R., S. Ullah, R. Ullah, I. U. Din, B. Kamal, M. A. H. Khan, and L. Matekovits, "Wideband and high gain array antenna for 5G smart phone applications using frequency selective surface," *IEEE Access*, Vol. 10, 86 117–86 126, 2022.

[9] Bameri, H. and O. Momeni, "A high-gain mm-Wave amplifier design: An analytical approach to power gain boosting," *IEEE Journal of Solid-state Circuits*, Vol. 52, No. 2, 357–370, Feb. 2017.

[10] Goudarzi, A., M. M. Honari, and R. Mirzavand, "A millimeter-wave resonant cavity antenna with multibeam and high-gain capabilities for 5G applications," *IEEE Transactions on Antennas and Propagation*, Vol. 70, No. 10, 9149–9159, Oct. 2022.

[11] Jeong, J.-M., H.-S. Bae, H. J. Lee, and J.-G. Lee, "Range enhancement of a 60 GHz FMCW heart rate radar using Fabry-Perot cavity antenna," *Electronics*, Vol. 14, No. 20, 4014, 2025.

[12] Trentini, G. V., "Partially reflecting sheet arrays," *IRE Transactions on Antennas and Propagation*, Vol. 4, No. 4, 666–671, Oct. 1956.

[13] Konstantinidis, K., A. P. Feresidis, and P. S. Hall, "Multilayer partially reflective surfaces for broadband Fabry-Perot cavity antennas," *IEEE Transactions on Antennas and Propagation*, Vol. 62, No. 7, 3474–3481, Jul. 2014.

[14] Qin, F., S. S. Gao, Q. Luo, C.-X. Mao, C. Gu, G. Wei, J. Xu, J. Li, C. Wu, K. Zheng, and S. Zheng, "A simple low-cost shared-aperture dual-band dual-polarized high-gain antenna for synthetic aperture radars," *IEEE Transactions on Antennas and Propagation*, Vol. 64, No. 7, 2914–2922, 2016.

[15] Gardelli, R., M. Albani, and F. Capolino, "Array thinning by using antennas in a Fabry-Perot cavity for gain enhancement," *IEEE Transactions on Antennas and Propagation*, Vol. 54, No. 7, 1979–1990, Jul. 2006.

[16] Liu, Y.-T., Y.-H. Yu, Y.-X. Sun, J. Ren, Y. Hou, H.-Q. Ma, and W. Wu, "1-D wide-angle scanning phased array with enhanced gain and reduced mutual coupling using thin dielectric superstrate," *IEEE Transactions on Circuits and Systems II: Express Briefs*, Vol. 71, No. 7, 3303–3307, 2024.

[17] Luo, W., X. Wang, X. He, and Y. Yang, "High gain dual-frequency dual-circularly polarized Fabry Perot resonant cavity antenna for Ku band," *Progress In Electromagnetics Research Letters*, Vol. 125, 1–7, 2025.

[18] Zhang, J. and H. Wong, "A high-gain millimeter-wave Fabry-Perot cavity antenna with phase correction on a meta-ground reflective surface," *IEEE Transactions on Antennas and Propagation*, Vol. 72, No. 8, 6187–6194, Aug. 2024.

[19] Zhang, X., C. Chen, S. Jiang, Y. Wang, and W. Chen, "A high-gain polarization reconfigurable antenna using polarization conversion metasurface," *Progress In Electromagnetics Research C*, Vol. 105, 1–10, 2020.